JOURNAL OF CATALYSIS 49, 294–304 (1977)

A Molecular Orbital Calculation of Adsorption of Ethylene and Acetylene on Nickel Cluster

HISAYOSHI KOBAYASHI,* HIROSHI KATO,† KIMIO TARAMA,* AND KENICHI FUKUI[1,*]

*Department of Hydrocarbon Chemistry, Faculty of Engineering, Kyoto University, Sakyo-ku, Kyoto 606, Japan; and †Department of General Education, Nagoya University, Chikusa-ku, Nagoya 464, Japan

Received December 31, 1976

The adsorption of ethylene and acetylene on a nickel surface has been investigated by applying the CNDO/2 method to the "surface molecule" model. The weakening of the C–C bond and the formation of a Ni–C bond, to which the s- and p-orbitals of a nickel atom make the major contribution as the result of adsorption, are discussed. The probability of a C–H bond fission and a Ni–H bond formation is small. The models used correspond to the initially formed surface species at low temperatures. The stronger adsorption of acetylene than that of ethylene is obtained, and this result agrees with experimental results. The interaction between the cluster and adsorbate is analyzed in terms of the orbital interactions.

INTRODUCTION

The concept of a "surface molecule," which consists of an adsorbed molecule and a small number of metal atoms (*1*), has been used to investigate the local characteristics of chemisorption. Several molecular orbital (MO) studies on chemisorption with a "surface molecule" model have been carried out with respect to simple adsorbate–adsorbent systems composed of an atom or a diatomic molecule and transition metal atoms (*2*). For the polyatomic molecules, however, quantum chemical approaches have scarcely been made in spite of the existence of much thermodynamic and spectroscopic data (*3*).

Recently, Rösch and Rhodin (*4*) studied the system composed of an ethylene molecule and two nickel atoms by employing the SCF-Xα scattered wave method (*5*). But the "surface molecule" used by them contains only two nickel atoms. The distance between ethylene and nickel atoms was fixed, and the structural change of adsorbed ethylene was also neglected. In addition adsorption energies were not discussed.

Another study of this system was made by Anderson (*6*). He examined chemisorbed ethylene and acetylene on a Ni(111) surface using the modified extended Hückel method (*7*). He paid most attention, however, to adsorbate–adsorbate interactions and the CH fragmentation produced by the C–C bond fission.

In the present paper, we look into the electronic structures and adsorption energies as well as the possibility of occurrence of dehydrogenation in regard to the system composed of a model surface of nickel and adsorbed ethylene with several representative orientations. In relation to the dehydrogenation of the adsorbed ethylene, we further investigate the adsorption of

[1] To whom reprint requests should be addressed.

ISSN 0021-9517

acetylene using the same model for the metal surface.

The calculation is performed by the CNDO/2 method (*8, 9*). This method is expected to give more reasonable charge distributions and a more reasonable d-band width than the extended Hückel method (*10*) which is usually employed in these sort of calculations.

CALCULATION OF A MODEL CLUSTER

We chose a Ni(100) face for our cluster model calculations because this face gives rise to the strongest interaction with adsorbed ethylene. This face is inclined to cause more extensive cracking than the other faces with low Miller indices, and on this face there should be relatively less catalytic activity for the hydrogenation of ethylene (*11*). The model cluster employed represents the truncated surface near the adsorbate and consists of eight nickel atoms as shown in Fig. 1. The nearest neighbor distance is taken as being equal to the metallic value (2.5 Å) (*12*). Two central atoms, compared to six surrounding edge atoms, receive the edge effect to a lesser extent, because of the replacement of the semi-infinite metal surface by the limited number of atoms.

The parameters for the carbon and hydrogen atoms are those given by Pople and Beveridge (*8*). For the nickel atoms, Blyholder's values (*9*) are adopted. These values are tabulated in Table 1.

The calculated values of the electron densities of nickel atoms, the d-band width, and the energy of the highest occupied (HO) levels of the adsorbate-free cluster are shown in Table 2. The electron populations of each atomic orbital of the central nickel atoms are also tabulated in Table 2. The energy levels of the cluster are illustrated in Fig. 2. The Fermi level is taken as the energy of the HOMO (*9, 10*), and this value (−7.2 eV) is somewhat lower than the experimental value

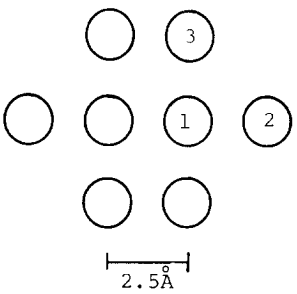

FIG. 1. The eight nickel atom cluster. The numbers in the circles represent atoms on different sites.

(ca. −5 eV) (*13*). This difference is rather small compared to the large difference between the HO levels calculated by the CNDO/2 method and the ionization potentials for usual organic compounds (*8*). Our preliminary extended Hückel calculation on the same cluster also gives the HO level (−7.8 eV) as close to the CNDO/2 result.

As shown in Fig. 2, the calculated d-bands are split into a few groups. In the present case, the d-band width is taken as the difference between the lowest and the highest groups of levels with a strong d-character (*9, 10*). Our calculated result (4.3 eV) is close to the experimental value (ca. 5 eV) (*14*), in spite of our simple model.

In the present model, eight nickel atoms are classified into three different sites as indicated in Fig. 1. A certain dissimilarity arises with respect to the charge distribution among nickel atoms; that is, the central atoms have less d-electron density and more s- and p-electron densities than edge atoms. Such differences are attributed to the edge effect which depends on shape and size of the model cluster used. The average value of d-electron densities in the cluster is 9.25, and this magnitude is less than the experimental value (9.4) for bulk nickel (*15*). Thus, judging from the above results, the cluster adopted here may sufficiently represent the surface of bulk nickel.

TABLE 1

The Parameters for the Nickel Atom (*9*)

CNDO/2	ζ	$\frac{1}{2}(Ip + E_A)$	β_A
3d	2.5	10.0	10.0
4s	1.8	4.3	6.0
4p	1.8	1.3	6.0

ETHYLENE ADSORPTION

Some ir studies have suggested that adsorbed ethylene on a nickle surface forms two σ C–Ni bonds (*16*, *17*). On the other hand, Demuth and Eastman suggest, by their uv photoemission (UPS) study (*18*), that the π-adsorbed ethylene interacts with a single nickel atom. (The two terms, "σ-diadsorbed" and "π-adsorbed," are used according to Ref. *18*). By the secondary ion mass spectrometry (SIMS), Barber *et al.* (*19*) found, at 77°K, two ionic species containing ethylene, that is, $NiC_2H^+_4$ and $Ni_2C_2H^+_4$.

The configurations of π-adsorbed and σ-diadsorbed ethylene with the planar structure (1.34 Å for the C–C and 1.07 Å for the C–H bond lengths) are illustrated in Fig. 3, where we refer to these as the A-type and the B-type, respectively.

We further adopted two configurations of adsorbed ethylene, where the molecule is deformed from a planar structure. These two configurations are also illustrated in Fig. 3 and are named the C- and D-types.

In the C-type, all four hydrogen atoms are equally bent above the C–C axis, and the structure of adsorbate resembles *cis*-didehydrogenated ethane. In the D-type, the methylenes in the C-type are rotated 120° with respect to one another around the C–C axis, and two C–H bonds are in the plane perpendicular to the cluster plane. Further, the C–C axis of ethylene inter-

FIG. 2. The energy levels of the cluster. Dark bands represent the group of energy levels. All levels except a few have a strong d-character.

TABLE 2

The Electron Densities of Nickel Atoms with Populations on Each Atomic Orbital of the Central Atoms, d-Band Width, and HOMO Level of the Cluster

Ni 1[a]	
d_{xz}	2.00
d_{yz}	2.00
d_{xy}	1.99
$d_{x^2-y^2}$	0.97
d_{z^2}	1.92
d-total	8.87
s	0.68
p_x	0.26
p_y	0.21
p_z	0.01
p-total	0.48
Ni 2[a]	
d-total	9.33
s	0.46
p-total	0.12
Ni 3[a]	
d-total	9.41
s	0.45
p-total	0.17
d-band width (eV)	4.30
HOMO level (eV)	−7.20

[a] Identification of Ni atoms in Fig. 1.

sects the X-axis at 30°. In the C- and D-type configurations, the C–C and C–H bonds make use of the distances in the ethane molecule: 1.54 Å for the C–C bond and 1.09 Å for the C–H bond.

Figure 4 gives the values of adsorption energies for the A-, B-, and C-types at various distances (R) between the C–C bond axis and the cluster plane. The equilibrium distances in the A-, B-, and C-types are obtained about 1.70, 1.85, and 1.70 Å, respectively. The A-type shows the largest adsorption energies among them at each R value. The adsorption energies of the D-type are much less than those of the B- or C-type (ca. 0.5 eV) and hence are omitted here.

The changes in the strength of the C–C, C–H, Ni–C, and Ni–H bonds when the adsorbate approaches the cluster are estimated from the corresponding changes in the E_{AB} values proposed by Pople and Beveridge (*8*). These E_{AB} values of the A- and B-types are shown in Fig. 5(a), and in Fig. 5(b), those of the C-type together with the B-type are shown.

In all cases, the weakening of C–C and C–H bonds and the formation of a Ni–C bond occur in the region of stronger interaction. Especially the s- and p-orbitals of nickel atoms make the major contribution to the formation of a Ni–C bond.

As shown in Fig. 5(a), the weakening of the C–C bond and the formation of a Ni–C bond occur more easily in the A-type interaction. But the extent of the weakening of the C–H bond in the B-type is a little larger than that in the A-type. As for the Ni–H bond formation, the E_{AB} values of the Ni–H bond in the A- and B-types are tabulated in Table 3 in the region near the equilibrium distances. For the B-type, all four Ni–H interactions are equivalent, and two central nickel atoms in the cluster make the major contribution. (See Fig. 3). In the case of the A-type, the Ni–H bond formation mainly includes three nickel atoms as shown in the diagram in Table 3,

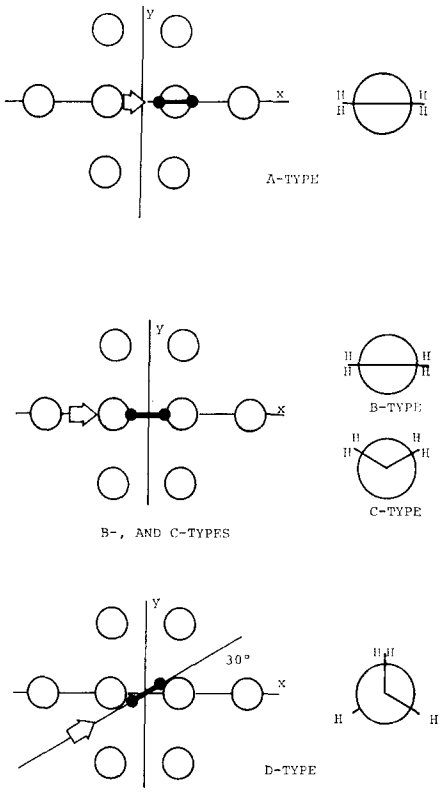

FIG. 3. The configurations of the π-adsorbed ethylene and of the σ-diadsorbed ethylene on the cluster. Eight nickel atoms and two carbon atoms with the C–C bond axis are illustrated on the left. The arrow shows the direction of the Newman projection on the right.

and four different interactions occur. We easily recognize that the extent of the formation of Ni–H bond is greater in the B-type, and this tendency is consistent with the result that the weakening of the C–H bond is greater in the B-type.

Comparing the E_{AB} values in the B-type with those in the C-type in Fig. 5(b), we find that the carbon atoms in the C-type interact more strongly with the nickel atoms than in the B-type, but the extents of C–H bond fission and Ni–H bond formation are greater in the latter.

For the D-type, we also examined the interaction between ethylene and the cluster, and the E_{AB} values of each bond are tabulated in Table 4.

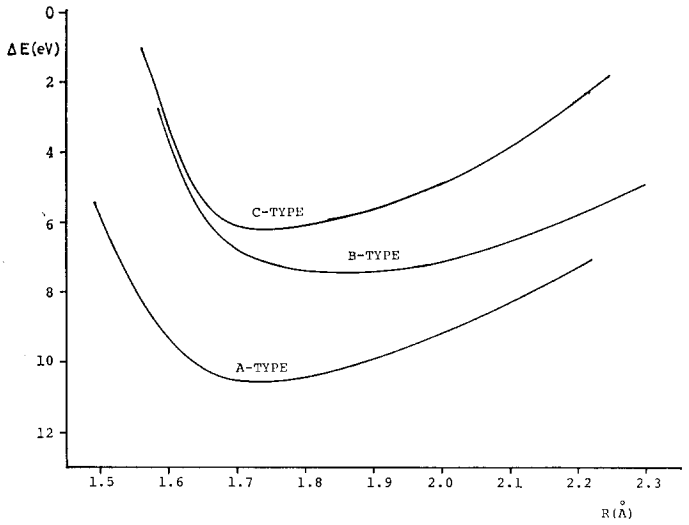

FIG. 4. The change in adsorption energies with the perpendicular distance (R) between ethylene and the cluster. The adsorption energies (ΔE) are calculated as follows: $\Delta E = -[$(total energy of surface molecule) − (total energy of free cluster) − (total energy of free ethylene in the planar structure)].

Besides the same tendencies as those in the A-, B-, and C-types, that is, the C–C and C–H bond weakening and the Ni–C and Ni–H bond formation on approach of the adsorbate, we see that the two C–H bonds in ethylene are drastically weakened while the other two C–H bonds virtually do not vary their strengths. We intend to discuss these results in some detail later.

As stated above, the carbon atoms in the A- and C-types interact more strongly with nickel atoms than those in the B-type. The

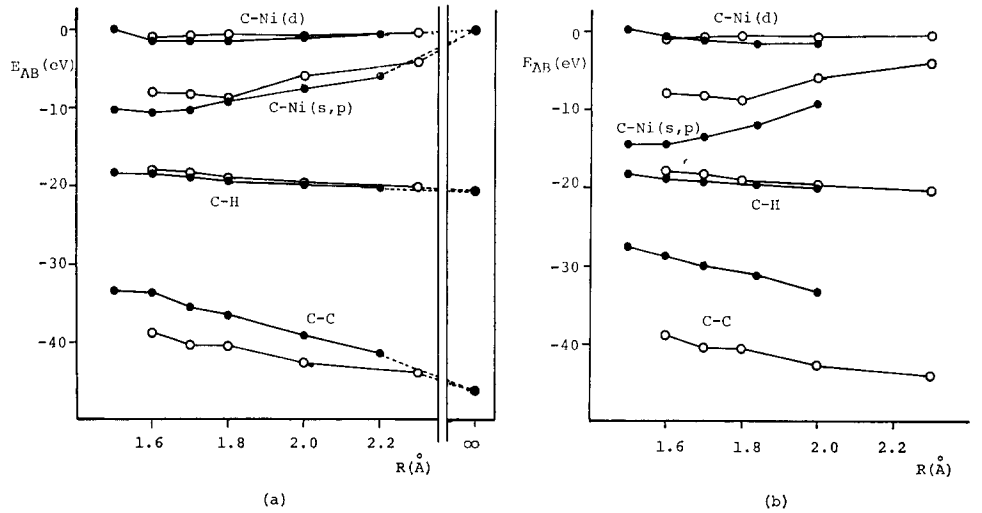

FIG. 5. Change of bond strengths for the A-, B-, and C-types with the distance (R). More negative values of E_{AB} mean stronger bonds. (a), A-Type (full circle) and B-type (open circle); (b), C-type (full circle) and B-type (open circle). The values of free ethylene are plotted in (a) as $R = \infty$.

TABLE 3

The E_{AB} Values of Ni–H Bonds in the A- and B-Types

R(Å)	A-type						B-type
	1	2	3	4	1 + 2	3 + 3	
1.6	−0.72	−0.30	−0.35	−0.83	−1.02	−1.18	−1.49
1.7	−0.49	−0.28	−0.29	−0.64	−0.76	−0.93	−.139
1.8	−0.38	−0.27	−0.26	−0.53	−0.65	−0.79	−1.15

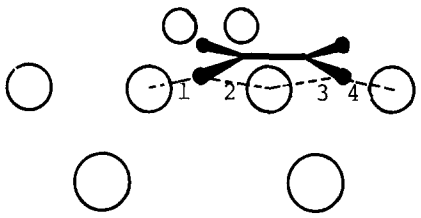

Identification of four different Ni–H interactions in the A-type

attractive interaction between hydrogen and nickel, however, is larger in the B-type than in the A- and C-types.

Comparing the A- and B-types, the latter has both smaller Ni–C and Ni–H bond lengths for the same R value, but the stronger Ni–C bond is formed in the former. Therefore this cannot be ascribed simply to the geometrical factor in these configurations. As to the Ni–H bond formation, a little stronger bond is formed in the B-type as expected from the smaller Ni–H bond length.

The C-type, in comparison with the B-type, has smaller Ni–C distances because of the 1.54-Å C–C bond length and larger Ni–H distances because the four hydrogen atoms are bent up.

Another reason for which the Ni–C interaction is stronger in the C-type relates to the electronic factor; namely, in the C-type interaction the orbital lobes of ethylene can more effectively overlap with the nickel atom orbitals owing to their sp^3 hybridization.

Generally, adsorption energies by the CNDO/2 method including metal d-orbitals are calculated to be much larger than the experimental values. For example, the calculated values of CO chemisorbed on a nickel surface are 3.5–8.4 eV (*20*), whereas the experimental ones are 1.4–2 eV (*21*). In the present case, the values given in Fig. 4 also appear too large compared with the experimental value of 2.5 eV (*22*). Thus, only relative values would be meaningful in the comparison of the adsorp-

TABLE 4

The E_{AB} Values in the D-Type

R(Å)	1.87	1.67	1.47
C–C	−29.27	−28.03	−26.60
C–H_1	−17.80	−16.74	−15.71
C–H_2	−20.35	−20.37	−20.36
Ni_1–C	−10.28	−10.65	− 9.11
Ni_1–H_1	− 0.55	− 0.82	− 0.98
Ni_2–H_1	− 0.73	− 1.02	− 1.21
(Ni_1 + Ni_2)–H_1	− 1.28	− 1.84	− 2.19

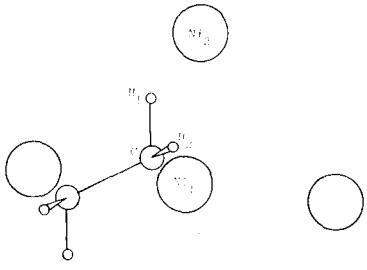

tion energies by such calculations with the experimental data.

It is somewhat unexpected that the stability in the C-type configuration is less than in the B-type. However, this could be ascribed to the overestimation of the deformation in ethylene molecule. Therefore we calculated the intermediate configuration between the B- and C-types with $R = 1.70$ Å. The resulting adsorption energy is 6.9 eV, and this value is larger than that in the C-type and even larger than that in the B-type with $R = 1.70$ Å. The E_{AB} values of each bond in the intermediate configuration lie between those in the B- and C-types.

It has been amply demonstrated that the fission of the C–H bonds (dehydrogenation of ethylene) may occur on adsorption. We also studied the possibility of C–H bond fission in adsorbed ethylene for the A-, B-, C-, and D-types. As illustrated in Fig. 5, the E_{AB} values of the C–H bond among the A-, B-, and C-types are almost the same, and weakening of the bond is scarcely suggested for these types.

However, from Table 4 we see that in the D-type the C–H bonds significantly weaken, and also, there is an extensive formation of Ni–H bonds, as suggested by Rye (*23*) in the case of ethylene adsorption on tungsten.

In this manner the D-type configuration is considered to be most favorable for the dehydrogenation reaction in spite of its smaller adsorption energy, and in the A-, B-, and C-types with large adsorption energies, the fission of C–H bonds does not occur easily. This result means that our calculations just correspond to the first species formed after the adsorption under very low temperatures, where little dehydrogenation occurs as suggested by UPS and ir spectroscopic studies (*16*, *18*).

We further refer to the ir spectroscopic study by Morrow and Sheppard (*16*). They observed the spectra of ethylene adsorbed on silica-supported nickel and assigned the bands at 2925, 2870, and 2790 cm^{-1} to the initially formed σ-diadsorbed species. The first two bands are asymmetrical and symmetrical CH_2 stretching modes and correspond to the bands at 3105.5 and 3019.3 cm^{-1} in free ethylene, respectively (*24*). The third is ascribed to an overtone of CH_2 deformation vibration and may be correlated with the band at 2880.1 cm^{-1} in free ethylene.

These shifts in frequency may be large compared to the adsorption shift on silica, approx. 10 cm^{-1}. Nevertheless the weakening of the C–H bonds is not drastic, and the C–H bond still exists in the CH_2 form. This is in accordance with our calculated results in which the weakening of this bond is small in the A-, B-, and C-types.

The existence of the associatively adsorbed species is also supported by the SIMS study already mentioned (*19*). From the relative values of calculated adsorption energies, though they are probably three or four times as high as the actual adsorption energy, we suggest that σ-diadsorbed ethylene in the B- or C-type and π-adsorbed ethylene will coexist at least at low temperature, and the amount of the latter is larger. These suggestions are in good agreement with the result by the SIMS that the amount of $NiC_2H^+_4$ is larger than that of $Ni_2C_2H^+_4$.

Dehydrogenation reactions of ethylene prevail for the adsorption at room temperature. Even at that temperature the electronic structure of the "surface molecule" may not vary from that under low temperatures. We interpret the A-type and the B- or C-type as the stable intermediates which may be detectable by differences in spectrometry, and the D-type as a transition state. The dehydrogenation reactions possibly proceed via this kind of deformed configuration (as a transition state) and produce acetylene in which the two C–H bonds bend up from the cluster plane.

To investigate the effect of deformed configurations on adsorption, we used only the σ-diadsorbed types. For the π-adsorbed

ethylene, a series of calculations on the deformed configurations may be carried out. But the elongation of C–C bond or the bending up of C–H bonds like those in the σ-diadsorbed types seems more disadvantageous in the π-adsorbed type because of the lengthened Ni–C and Ni–H distances. Therefore we did not calculate adsorption energies and bond strengths regarding these configurations. However, we could say without further calculations that the σ-diadsorbed types would play the major role in the dehydrogenations, though adsorption energies are largest in the A-type.

In order to analyze the mode of orbital interaction between ethylene and the cluster, we expanded the MOs of the combined system of adsorbate and adsorbent using linear combinations of both the MOs of free ethylene and free cluster. The MO expansion coefficients are calculated for the A- and B-types. We only pay attention to the mixing between unoccupied MOs and occupied MOs of ethylene and the cluster which are more important than others (*25*). The most typical orbital interactions are in the B-type and their respective expansion coefficients are illustrated in Fig. 6. Figure 6(a) shows the mode of electron delocalization to the π^* orbital in ethylene from two MOs with strong d-character in the cluster. This interaction serves to bring about the weakening of the C–C bond. It is seen from Fig. 6(b) that the mixing of π and pσ orbitals of ethylene and an unoccupied MO with strong p-character in the cluster causes a reverse charge transfer and also the remarkable lowering of the orbital energy.

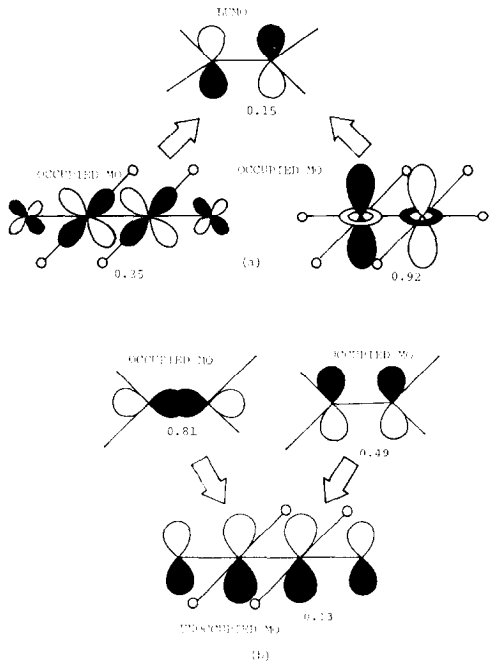

FIG. 6. Typical mode of mixing of MOs between ethylene and the cluster for the B-type. (a), The lowest unoccupied MO (LUMO) of ethylene and occupied MOs of the cluster; (b), occupied MOs of ethylene and unoccupied MO of the cluster. Arrows show the direction of the charge transfer. The figures shown under each MO diagram are the MO expansion coefficients of the ethylene–cluster system by the MOs of the ethylene molecule and the cluster, with their phases taken as indicated.

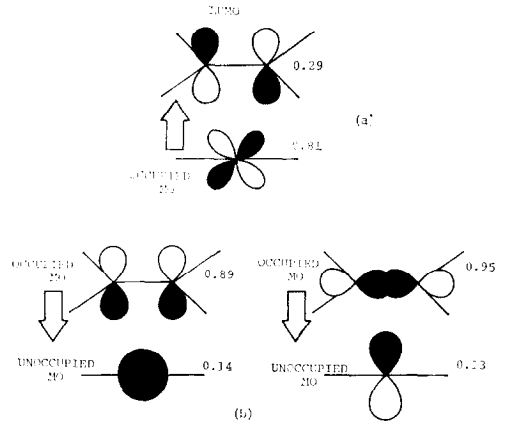

FIG. 7. Typical mode of mixing of MOs between ethylene and the cluster for the A-type. Refer to the caption of Fig. 6 for the detailed notations.

In the case of the A-type, a similar but slightly different mode of orbital interaction is seen. The mode is illustrated in Fig. 7. We find that the electron delocalization to the π^* orbital is mainly due to the d_{xz} cluster orbital, and the π and pσ orbitals in free ethylene mix with the cluster ones composed of s and p_z atomic orbitals.

These orbital interaction modes are reasonable if one recalls the electron popu-

TABLE 5

The Changes in E_{AB} Values of the Adsorbed Acetylene for the Bending Angle θ in the E-Type and F-Type

	Type: θ							C_2H_2[b]
	E: 0°	E: 30°	E: 60°	E: −30°[a]	F: 0°	F: 30°	F: 60°	
E_{AB} C–C	−52.19	−49.75	−44.98	−52.52	−56.20	−54.20	−48.03	−62.84
C–H	−19.71	−20.14	−19.62	−17.44	−18.64	−19.27	−18.75	−21.39
Ni–C	−10.91	−11.91	−12.97	− 9.46	− 8.54	− 9.40	−12.84	
Ni–H	− 0.95	− 0.27	0	− 1.41	− 1.84	− 0.92	0	

[a] Two C–H bonds are bending toward the cluster.
[b] The values of free acetylene.

lation on the central nickel atoms in Table 2. The d-orbitals are almost filled with two electrons except for $d_{x^2-y^2}$ orbital which is occupied by one electron. In particular we pay attention to the nodal property of the central two d^2_z orbitals on the cluster for the B-type. Since each d^2_z orbital is occupied by two electrons, both bonding (in phase) and antibonding (out of phase) cluster orbitals composed of these d^2_z orbitals are doubly occupied ones.

Therefore we can assume that the π-orbital in ethylene does not cause an attractive interaction with the d^2_z cluster orbitals because interactions between occupied orbitals lead to instability. This interaction mode is sketched as follows. The

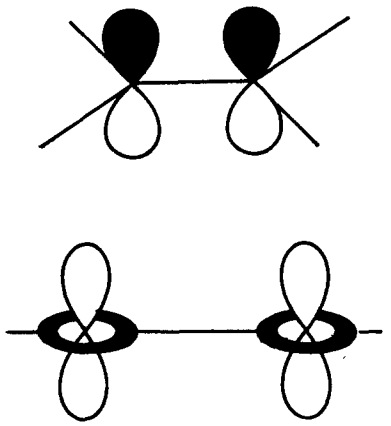

π-orbital in ethylene may only interact with unoccupied orbitals which are in phase on the central nickel atoms, and the cluster orbitals composed of s- or p-atomic orbitals are available as illustrated in Fig. 6.

In the A-type, the same explanation as that in the B-type is given: The π-orbital does not interact with the nearest d^2_z orbital accompanying any stabilization as sketched below, but interacts with s- and p-orbitals as shown in Fig. 7.

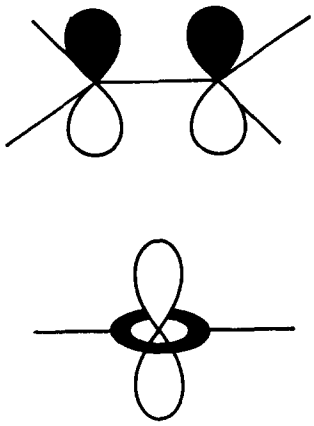

These are the reasons why the s- and p-orbitals make the major contribution to the formation of Ni–C bonds. Though the interactions between π and π^* MO in ethylene and the s- and p-orbitals on the cluster are somewhat overestimated in our calculations, we are sure that the contribution from the unoccupied s- and p-orbitals of nickel are considerably large especially in adsorption of electropositive molecules such as ethylene or acetylene.

In both cases mentioned above, six

occupied MOs in a free ethylene molecule are still localized in the adsorbate in the course of adsorption. As shown in Fig. 6(b) and Fig. 7(b), the C–C σ and π bonds, however, considerably mix into each other through the interactions of the cluster orbital, although experimental information (*18*) indicates that the degree of mixing may be overestimated. All of the localized MOs in ethylene are more or less stabilized when adsorbed, so the stabilization of the π-orbital is particularly remarkable and mainly contributes to increase the adsorption energy.

ACETYLENE ADSORPTION

We also studied the adsorption of acetylene fixing the C–C axis parallel to the cluster plane and using 1.20 Å for the C–C and 1.06 Å for the C–H bond length. We examined both the π-adsorbed (E-type) and σ-diadsorbed (F-type) acetylene 1.80 Å above the surface as illustrated in Fig. 8. The angle θ is defined as the inclination of the C–H bond from the C–C axis (also shown in Fig. 8). The adsorption energies and the E_{AB} values of linear and bent structures are shown in Fig. 9 and Table 5, respectively. The calculations were carried out for the three bent structures (θ = 30, 60, and −30°) of the E-type, and also for

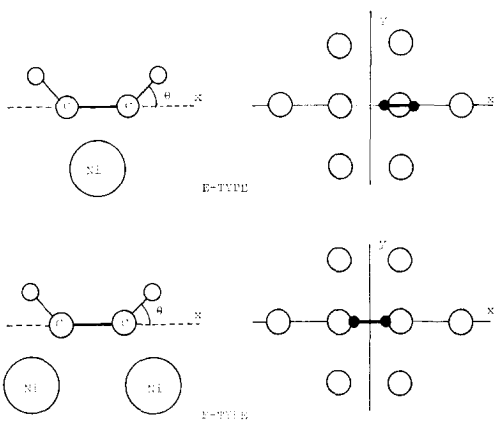

FIG. 8. The orientations of the adsorbed acetylene for the π-adsorbed (E) type and the σ-diadsorbed (F) type.

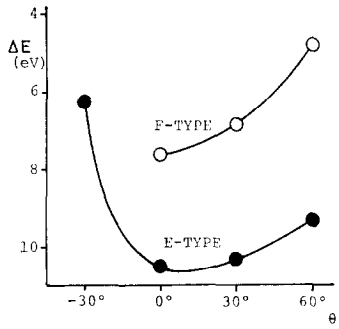

FIG. 9. The change in acetylene adsorption energies (ΔE) with the angle θ. Here, ΔE is taken in a manner similar to that in the case of ethylene.

the two (θ = 30 and 60°) of the F-type. The bent structure with θ = −30° in the F-type, where nickel atoms and hydrogen atoms in close proximity, was not examined.

Comparing the E_{AB} values obtained for two types, the general trend of change in each bond strength is the same as in the case of ethylene adsorption; that is, the C–C bond weakening and the C–Ni bond formation in the E-type are greater, and in the F-type the C–H bond weakening and the Ni–H bond formation are greater than in another type.

As for the adsorption energies, larger values are obtained in the E-type, and this tendency is the same as in the case of ethylene. Moreover, the linear structure is most stable in both types. In the E-type, the difference in the adsorption energies in θ = 0° and θ = 30° is especially small, but the structure with θ = −30° is much more unstable than the linear one. This means that the bending up of the C–H bonds probably occurs in some degree, but the bending down toward the cluster which was suggested by Ito using the extended Hückel method will not occur (*26*).

We next compare the E_{AB} values and the adsorption energies for the acetylene adsorption in θ = 0° with those for the case of ethylene. The C–H bonds in the E- and F-types are stronger than those in the A- and B-types, respectively, and the adsorption energies for the E- and F-types are

larger than the values in corresponding types of ethylene.

These results indicate that acetylene is more stable to dehydrogenation and is adsorbed more strongly than ethylene. These tendencies are in good agreement with experimental results, which show that adsorbed ethylene can change to acetylene and acetylene will not be desorbed or decomposed up to higher temperatures (470°K), whereas ethylene would be decomposed at lower temperatures (230°K) (*18*, *22*).

ACKNOWLEDGMENTS

One of the authors is grateful to Kazuyoshi Tanaka and Tsutomu Minato for their helpful advice and discussion. The authors thank the Data Processing Center of Kyoto University for generous use of the FACOM 230-60/75 computer.

REFERENCES

1. Grimley, T. B., "Molecular Processes on Solid Surfaces," p. 299. McGraw-Hill, New York, 1969.
2. Anders, L. W., and Hansen, R. S., *J. Chem. Phys.* **62**, 1641 (1975); Blyholder, G., *J. Chem. Phys.* **62**, 3193 (1975); Anderson, A. B., and Hoffmann, R., *J. Chem. Phys.* **61**, 4545 (1974); Baetzold, R. C., *Surface Sci.* **51**, 1 (1975).
3. Morgan, A. E., and Somorjai, G. A., *J. Chem. Phys.* **51**, 3309 (1969); McKee, D. W., *J. Amer. Chem. Soc.* **84**, 1109 (1962); Plummer, E. W., Waclawski, B. J., and Vorburger, T. V., *Chem. Phys. Lett.* **28**, 510 (1974).
4. Rösch, N., and Rhodin, T. N., *Faraday Spec. Discuss. Chem. Soc.* **58**, 28 (1974).
5. Slater, J. C., and Johnson, K. H., *Phys. Rev.* **B5**, 844 (1972).
6. Anderson, A. B., *J. Chem. Phys.* **65**, 1729 (1976).
7. Anderson, A. B., *J. Chem. Phys.* **62**, 1187 (1975). For the extended Hückel method, see Hoffman, R., *J. Chem. Phys.* **39**, 1397 (1963).
8. Pople, J. A., and Beveridge, D. L., "Approximate Molecular Orbital Theory." McGraw-Hill, New York, 1970.
9. Blyholder, G., *Surface Sci.* **42**, 249 (1974).
10. Fassaert, D. J. M., Verbeek, H., and Van der Avoird, A., *Surface Sci.* **29**, 501 (1972).
11. Dalmai-Imelik, G., and Massardier, J., "The Sixth International Congress on Catalysis." London, 1976.
12. "Tables of Interatomic Distances and Configuration in Molecules and Ions." The Chemical Society, London, 1965.
13. Farnsworth, H. E., and Madden, H. H., *J. Appl. Phys.* **32**, 1933 (1961); Gerlach, R., and Rhodin, T. N., "The Structure and Chemistry of Solid Surface." Wiley, New York, 1969.
14. Eastman, D. E., and Krolikowski, W. F., *Phys. Rev. Lett.* **21**, 623 (1968).
15. Blodgett, A. J., Jr., and Spicer, W. E., *Phys. Rev.* **146**, 390 (1966).
16. Morrow, B. A., and Sheppard, N., *Proc. Roy. Soc. A* **391** (1969).
17. Erkelens, J., and Liefkens, Th. J., *J. Catal.* **8**, 36 (1967); Little, L. H., Sheppard, N., and Yates, D. J. C., *Proc. Roy. Soc. A* **259**, 242 (1960).
18. Demuth, J. E., and Eastman, D. E., *Phys. Rev. Lett.* **32**, 1123 (1974), *Phys. Rev.* **B13**, 1532 (1976).
19. Barber, M., Vickerman, J. C., and Wolstenholme, J., *J. Catal.* **42**, 48 (1976).
20. Blyholder, G., *J. Phys. Chem.* **79**, 756 (1975).
21. Tracy, J. C., *J. Chem. Phys.* **56**, 2736 (1972); Ford, R. R., *Adv. Catal.* **21**, 51 (1970).
22. Bond, G. C., "Catalysis by Metals." Academic Press, New York, 1962.
23. Rye, R. R., *Acc. Chem. Res.* **8**, 347 (1975).
24. Herzberg, G., "Molecular Spectra and Molecular Structure II. Infrared and Raman Spectra of Polyatomic Molecules." Van Nostrand, London, 1945.
25. For instance, see Fukui, K., "Theory of Orientation and Stereo Selections." Springer-Verlag, Berlin, 1975.
26. Ito, H., *Shokubai* **17**, 141 (1975).